

# Digital Control for Power Flow Management in a PV System Supplying DC loads

M.Karthikaa<sup>1</sup> | Dr.R.Subramaniam<sup>2</sup> | C.Ramakrishnan<sup>3</sup>

<sup>1</sup>(PG Scholar, EEE Department, SNS college of Technology, Coimbatore, India.kaarthi136@gmail.com)

<sup>2</sup>(Professor & Dean, EEE Department, SNS college of Technology, Coimbatore, India,rame.smani@gmail.com)

<sup>3</sup>(AP(SG),EEE Department, SNS college of Technology, Coimbatore, India, ramramki.krishnan@gmail.com)

**Abstract**--The photovoltaic (PV) system is efficacious and thus has universal employment like the usage of LED-based street lights, electronic chokes, and compact fluorescent lamps in this machinery world. The system under study is a grid connected PV system supported by a battery, supplying DC loads which is directly connected to the DC bus. As multiple sources (PV, battery, grid) and sinks (battery, grid, DC loads) are included, a viable Power flow Management Strategy (PMS) is required to balance power flow. The PMS manages the multimode operation of bidirectional converter, battery charging and discharging cycle which enables a grid-friendly operation. MATLAB/SIMULINK software was used to simulate the proposed system. Finally, the objectives are validated through the simulation results to prove the effectiveness of the system.

**Index terms:** Bidirectional converter, Photovoltaic (PV), Power flow Management System (PMS)

## 1. INTRODUCTION

Fossil fuel was a major source of electricity in the past years. Due to continuous use of fossil fuel, it created detrimental greenhouse impacts on living beings. With the growing concern over environmental issues and the increasing usage of dc loads for low cost, PV based systems are employed in diverse applications.[1]

PV systems are broadly classified as stand-alone and grid connected systems [2], [3]. Stand-alone systems are popular in remote areas where electricity is not viable. The reliability of such systems is improved by usage of storage batteries [4]. Grid connected systems allows to reduce our consumption from grid and in some instances, to feed surplus energy back to grid, which may give credit for energy returned. The improvement of power electronics has a positive impact on the grid connected PV systems [5]-[13].

Various control strategies have been discussed in various literatures [7]-[18]. In Grid Connected PV systems (GCPV), generated power is fed to loads and grid. Widely battery is used to compensate the mismatch between generation and demand [19]. In addition, even during unscheduled short term outages battery plays a vital role. Therefore grid side inverter should operate in grid-tied and off-grid mode to supply critical loads during power outages [9].

The growing emphasis on energy saving has increased usage of LED-based street lights, electronic chokes, compact fluorescent lamps. PV being the most promising energy source

enables the dc loads to be connected directly to dc bus. In GCPVs, a major problem is that, variations in PV power will cause fluctuations in dc-link voltage. In the traditional method, ac line current is adjusted, which leads to poor power quality[20]. Moreover, when dc link voltage is disturbed, it is reflected in PV array power and PV operating point is shifted from maximum operating point(MPP). Hence a fast regulation of dc link voltage is achieved through a controller.

The proposed system consists of three power sources (grid, PV array and battery), three power sinks (grid, battery and load) and a power flow management system (PMS) to balance the power flow. In this paper, when PV power is more than the load demand; excess power is fed to the grid. Similarly when PV power is insufficient, grid will supply the load. Therefore, it provides uninterrupted power supply to dc loads, making the system reliable.

This paper is structured as follows. Section II gives a description of the system which includes the control strategy of the dc link voltage regulation and power flow management. Section III focuses on the overall simulation model. Section IV presents the simulation results of the proposed system. Finally, Section V presents the conclusion.

## 2. SYSTEM DESCRIPTION

The GCPV system consists of a PV array, a boost dc-dc converter, a battery storage unit with its charger/discharger circuit, and a bidirectional converter for interfacing with grid, and the schematic of the PV system is shown in Fig.1.

A boost converter embedding MPPT(Perturb and Observe Algorithm) tracks maximum power from the PV array, and a bidirectional dual active bridge converter (battery charger/discharger) operating in both buck and boost modes regulates the dc link voltage. The PV system focuses to provide an unremitting power supply to the loads connected at the dc side, and the grid is used as a backup means when there is insufficient PV power and complements the grid when excess PV power is available. This necessitates the bidirectional converter to operate in three operating modes, namely, idle mode (grid is disconnected), inverter mode, and rectifier mode.

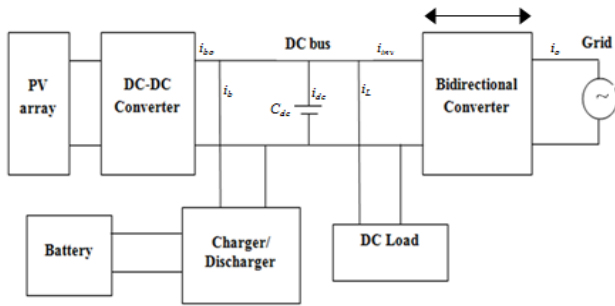


Fig.1. Grid-connected PV system with dc loads.

Based on the availability of the PV power and load demand, the battery is charged either from PV or the grid. The voltage control loop of the charger/discharger circuit defines the charging/discharging mode of the battery. The PV system involves energy sources (PV, battery, and grid), and sinks (battery, grid and dc load) therefore a PMS is required to balance the power flow among them. The various control methods are explicated in the further sections.

#### A. Dc Link Voltage Controller

In a grid-connected PV system with dc loads, the instantaneous power relationship is given by,

$$P_{bo}(t) = P_b(t) + P_{dc}(t) + P_L(t) + P_{inv}(t) \quad (1)$$

where  $P_{bo}$  is the output power of the boost converter,  $P_b$  is the power delivered by the charger/discharger circuit,  $P_{dc}$  is the power to the dc link capacitor,  $P_L$  is the power consumed by the dc load, and  $P_{inv}$  is the power extracted by the inverter. The instantaneous ac power can be written as

$$G_{dc}(s) = \frac{v_{dc}(s)}{d(s)} = \frac{(s + 2/r_s C_1)[(2d - 1)2V_1(3C_2 - C_1)]/(f_{sw} L C_1 C_2)}{s^2 + (2/r_s C_1 + 2/r_s C_1)s + 4/Rr_s C_1 C_2 + (2d^2 - 2d)^2/f_{sw}^2 L^2 C_1 C_2} \quad (9)$$

$$G_{vb}(s) = \frac{v_{dc}(s)}{V_b(s)} = \frac{(-2d^2 + 2d)2/(f L r_s C_1 C_2)}{s^2 + (2/r_s C_1 + 2/r_s C_1)s + 4/Rr_s C_1 C_2 + (2d^2 - 2d)^2/f^2 L^2 C_1 C_2} \quad (10)$$

$$P_{ac} = (V_m \sin \omega t)(I_m \sin \omega t) \quad (2)$$

$$= \frac{V_m I_m}{2} - \frac{V_m I_m}{2} \cos 2\omega t \quad (3)$$

where  $V_m$  is the amplitude of the phase voltage and  $I_m$  is the amplitude of grid current. The ac power includes a dc term and a second-order ripple in the dc voltage. The average power on the dc side can be written as

$$P_{inv} = V_{dc} I_{inv} \quad (4)$$

where  $I_{inv}$  is the average current on the dc side of the inverter. By equating the average power on the dc side and the dc term on the ac side, we get

$$\frac{V_m I_m}{2} = \eta V_{dc} I_{inv} \quad (5)$$

where  $\eta$  is the efficiency of the inverter. If  $V_{dc}$  and  $V_{dc(ref)}$  are the actual and reference values of dc link voltage, respectively, the change in energy ( $\Delta E_{dc}$ ) stored in the dc link capacitor  $C_{dc}$  can be written as

$$\Delta E_{dc} = \frac{C_{dc}}{2} (V_{dc(ref)}^2 - V_{dc}^2) \quad (6)$$

To inject the PV power to the grid while maintaining a constant  $V_{dc}$ , the following energy balance should be satisfied:

$$\Delta E_{dc} = T \left( p_{bo} - p_L - p_b - \frac{V_m I_m}{2\eta} \right) \quad (7)$$

where  $T$  is the time period of ac supply.

Combining (6) and (7)

$$V_{dc}^2 = V_{dc(ref)}^2 - \frac{2T}{C_{dc}} (p_{bo} - p_L) + \frac{2T}{C_{dc}} p_b + \frac{T}{C_{dc} \eta} V_m I_m \quad (8)$$

From (8), it is clear that the fluctuations in PV power due to the change in solar radiation and the load power cause variations in the dc link voltage. These disturbances in dc link voltage are again reflected in PV array power, which shifts the PV power from MPP. Therefore a fast regulation of dc link voltage is necessary. A charger/ discharger controller is designed as equation (8) in reference to [22] which are expressed below.

The control structure of the system is shown in Fig.2 where  $V_{dc}$  is regulated by the charger/discharger circuit.

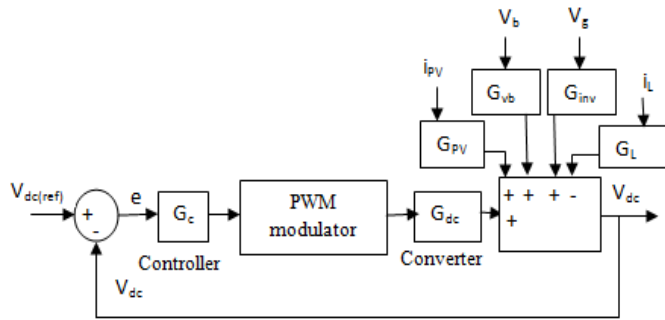


Fig.2. Control scheme of proposed system

The parameters used in the controller are shown in Table I

TABLE I  
PARAMETERS OF THE CONTROLLER

$r_s, R$	0.0024Ω, 30Ω
$C_1, C_2, C_{dc}$	1000μF, 1000μF, 1000μF
$L$	40μH
$V_1$	36V
$d, D$	0.1, 0.65
$f_{sw}$	10kHz
$T$	0.036s
$k, K_p, K_i$	1, 0.8, 0.01

The converter control to output transfer function  $G_{dc}$ [32] is expressed as (9), where  $r_s$  is the resistance of the battery,  $C_1$  and  $C_2$  are the input and output capacitances, respectively,  $L$  defines the leakage inductance of the transformer,  $f_{sw}$  is the switching frequency, and  $d$  is the phase shift between the two bridges of the converter.

The source to input transfer function [22] is given by (10). The transfer function of the load is represented by  $G_L$

$$G_L(s) = \frac{v_{dc}(s)}{I_L(s)} = -\frac{1}{C_{dc}(s+1/RC_{dc})} \quad (11)$$

where  $R$  is the equivalent resistance of the load, and the relation between PV current and the dc link voltage is expressed as

$$G_{pv}(s) = \frac{v_{dc}(s)}{I_{pv}(s)} = R(1 - D) \quad (12)$$

$G_{inv}$  denotes the transfer function of the grid connected inverter

$$G_{inv}(s) = \frac{k}{(1+s\tau)} = \frac{v_{dc}(s)}{V_g(s)} \quad (13)$$

where  $k$  is the amplitude gain and  $\tau$  is the sampling delay.

*B. Power Flow Management Strategy*

The main functions of PMS are, to monitor the battery voltage, to generate a mode selection signal for the bidirectional converter, and to generate the reference current for the hysteresis current controller.

The converter mode selection is done using predetermined double bands of battery voltages. The outer band corresponds to two voltage limits that correspond to the battery extreme voltages, i.e., the float value and deep discharge level as, the outer upper threshold voltage ( $V_{OUT}$ ) and the outer lower threshold voltage ( $V_{OLT}$ ). The transition from idle mode to conducting (rectifier/inverter) mode is based on the outer band limits.

Similarly, the inner band voltage limits, corresponding to interior voltage levels for the purpose of control i.e., the inner upper threshold voltage ( $V_{IUT}$ ) and the inner lower threshold voltage ( $V_{ILT}$ ). The inner band limits defines the changeover from conducting mode to idle mode.

The control strategy is based on the bands of battery voltage and previous mode of operation which dictates and the reference current value as shown in Table II.

TABLE II  
CONTROL STRATEGY FOR PMS

Case	Battery voltage $V_b$	Previous mode	Present mode
1	$V_b \leq V_{OLT}$	Idle	Rectifier
2	$V_{OLT} < V_b < V_{OUT}$	Idle	Idle
3	$V_b \geq V_{OUT}$	Idle	Inverter
4	$V_{ILT} < V_b < V_{OUT}$	Inverter	Inverter
5	$V_b \geq V_{OUT}$	Inverter	Inverter
6	$V_{OLT} < V_b \leq V_{ILT}$	Inverter	Idle
7	$V_{OLT} < V_b \leq V_{IUT}$	Rectifier	Rectifier
8	$V_b \leq V_{OUT}$	Rectifier	Rectifier
9	$V_{ILT} < V_b < V_{OUT}$	Rectifier	Idle

The control scheme for the implementation of PMS is shown in Fig.3. Based on the voltage threshold limits, two selection signals ( $S1, S0$ ) for the multiplexer are generated. The inputs for the multiplexer 0, 1, and  $-1$  which denotes the idle, rectifier, and inverter modes of operation, respectively. The selection signals will determine the mode ( $M$ ) of operation of the converter.

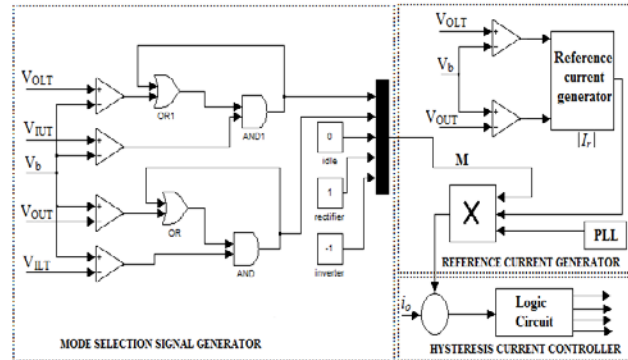


Fig.3. Control Scheme of the PMS.

Depending on the outer band limits of battery, a reference current is generated, which is fed to hysteresis current controller. Finally, the pulses generated are fed to the bidirectional converter module.

C.Hysteresis Current Controller

A hysteresis current controller is widely used in many industrial applications [22].

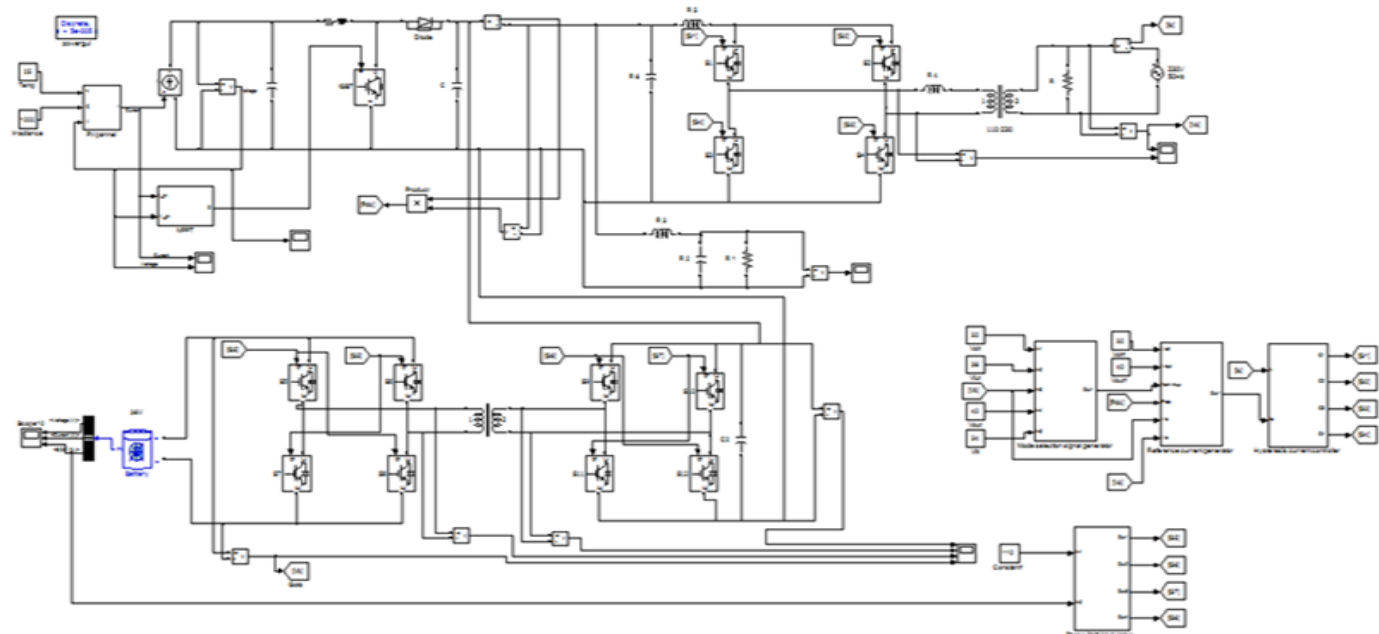


Fig. 5 Grid Connected PV system simulation model

3. SIMULATION MODEL

Its primary application is current control of an inverter. The scheme of a single-band hysteresis current controller is shown in Fig.4.

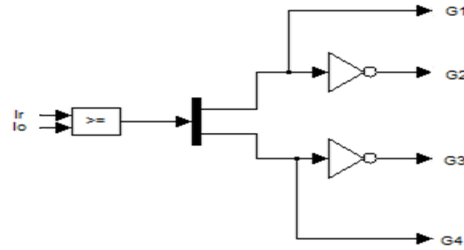


Fig.4. Hysteresis Current Controller

The reference signal for the hysteresis current controller is produced as a function of the phase of the grid voltage using Phase Locked Loop (PLL). A single-band hysteresis current controller is used. In this case, the inverter will generate a positive output voltage when the current error touches the lower hysteresis limit. On the other hand, a negative output voltage is produced when the current error reaches the upper hysteresis limit. Thus, producing pulses for the bidirectional converter.

The system consists of a PV array, a boost converter to extract maximum power from PV array, a bidirectional converter, and a bidirectional dc-dc converter circuit as charger/discharger circuit for the battery. The power flow management strategy provides an uninterrupted power supply to the loads connected at the dc side. Fig.5 shows the complete Simulink model of the proposed system.

4.RESULTS AND DISCUSSION

A.PV Module

The PV array is interfaced with the boost converter providing an output of 110 V as shown in Fig.6. In order to extract maximum power from PV array among different MPPT techniques, Perturb and observe (P&O) algorithm is used.

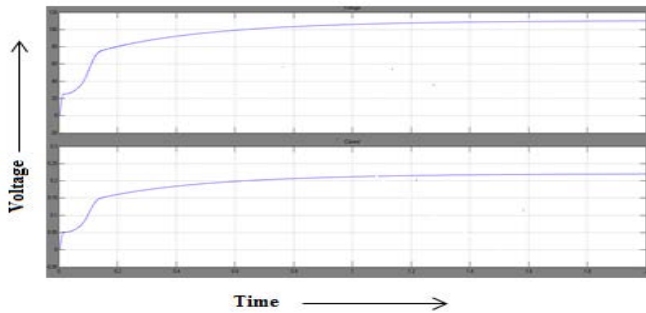


Fig.6 Output of PV module

B.Charger/Discharger Module

The system is supported by a battery interfaced with a bidirectional dual active bridge converter which can operate in either buck or boost mode acting as the charger/discharger circuit of the battery. Fig.7 explains the transition of modes vividly.

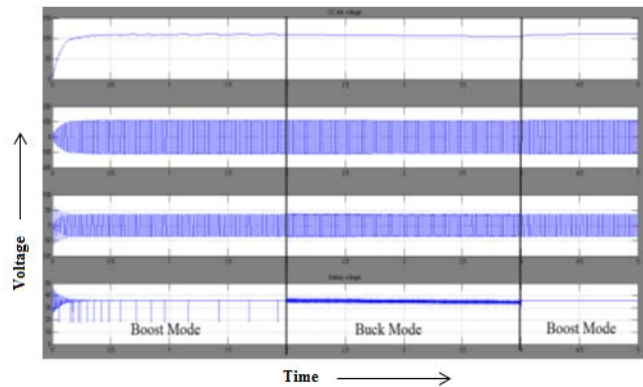


Fig.7 Transition between buck/boost mode

C.DC Load Voltage

The main aim of the system is to provide an uninterrupted power supply to the DC loads, when excess PV power is available, it supplies power to the load and when there is insufficient PV power, grid power is utilized. Fig.8 explicates the voltage across the DC load.

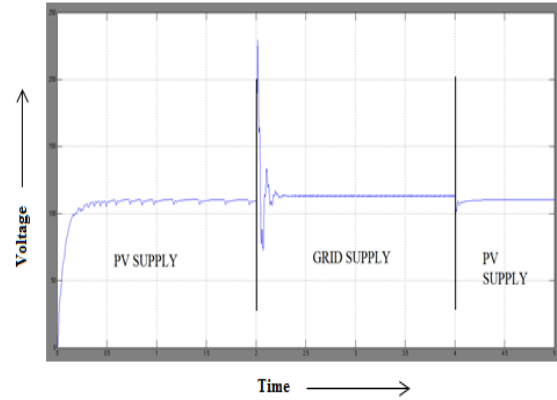


Fig.8 DC load voltage

5.CONCLUSION

A viable control strategy for power flow management in a grid-connected PV system feeding dc loads has been presented. The proposed configuration is attractive from the perspective of providing uninterruptible power to dc loads. A smooth transition of modes of the bidirectional converter is observed while ensuring that the excess PV power is supplied of high quality into the grid.

REFERENCES

- [1] Yazdani and P. P. Dash, "A control methodology and characterization of dynamics for a photovoltaic system interfaced with a distribution network," *IEEE Trans. Power Del.*, vol. 24, no. 3, pp. 1538-1551, Jul. 2009.
- [2] X. Q. Guo and W. Y. Wu, "Improved current regulation of three-phase grid-connected voltage-source inverters for distributed generation systems," *IET Renew. Power Gener.*, vol. 4, no. 2, pp. 101-115, Mar. 2010.
- [3] H. C. Chiang, T. T. Ma, Y. H. Cheng, J. M. Chang, and W. N. Chang, "Design and implementation of a hybrid regenerative power system combining grid-tie and uninterruptible power supply functions," *IET Renew.Power Gener.*, vol. 4, no. 1, pp. 85-99, Jan. 2010.
- [4] F. Giraud and Z. M. Salameh, "Steady-state performance of a gridconnected rooftop hybrid wind-photovoltaic power system with battery storage," *IEEE Trans. Energy. Convers.*, vol. 16, no. 1, pp. 1-7, Mar. 2001.
- [5] Y.-K. Lo, T.-P. Lee, and K.-H. Wu, "Grid-connected photovoltaic system with power factor correction," *IEEE Trans. Ind. Electron*, vol. 55, no. 5, pp. 2224-2227, May 2008.
- [6] Y. K. Lo, H. J. Chiu, T. P. Lee, I. Purnama, and J. M. Wang, "Analysis and design of a photovoltaic system connected to the utility with a power factor corrector," *IEEE Trans. Ind. Electron.*, vol. 56, no. 11, pp. 4354-4362, Nov. 2009.
- [7] R. A. Mastromauro, M. Liserre, T. Kerekes, and A. Dell' Aquila, "A single-phase voltage-controlled grid-connected photovoltaic system with

- power quality conditioner functionality," *IEEE Trans. Ind. Electron.*, vol. 56, no. 11, pp. 4436–4444, Nov. 2009.
- [8] J. M. Espí, J. Castelló, R. García-Gil, G. Garcerá, and E. Figueres, "An adaptive robust predictive current control for three-phase grid-connected inverters," *IEEE Trans. Ind. Electron.*, vol. 58, no. 8, pp. 3537–3546, Aug. 2011.
- [9] Z. Yao, L. Xiao, and Y. Yan, "Seamless transfer of single phase gridinteractive inverters between grid connected and standalone modes," *IEEE Trans. Power Electron.*, vol. 25, no. 6, pp. 1597–1603, Jun. 2010.
- [10] J.-M. Kwon, B.-H. Kwon, and K.-H. Nam, "Grid-connected photovoltaic multistring PCS with PV current variation reduction control," *IEEE Trans. Ind. Electron.*, vol. 56, no. 11, pp. 4381–4388, Nov. 2009.
- [11] S. Yang, Q. Lei, F. Z. Peng, and Z. Qian, "A robust control scheme for grid-connected voltage-source inverters," *IEEE Trans. Ind. Electron.*, vol. 58, no. 1, pp. 202–212, Jan. 2011.
- [12] Y.-C. Kuo, T.-J. Liang, and J.-F. Chen, "Novel maximum power point tracking controller for photovoltaic energy conversion system," *IEEE Trans. Ind. Electron.*, vol. 48, no. 3, pp. 594–601, Jun. 2001.
- [13] Y.-K. Lo, T.-P. Lee, and K.-H. Wu, "Grid-connected photovoltaic system with power factor correction," *IEEE Trans. Ind. Electron.*, vol. 55, no. 5, pp. 2224–2227, May 2008.
- [14] Y. K. Lo, H. J. Chiu, T. P. Lee, I. Purnama, and J. M. Wang, "Analysis and design of a photovoltaic system connected to the utility with a power factor corrector," *IEEE Trans. Ind. Electron.*, vol. 56, no. 11, pp. 4354–4362, Nov. 2009.
- [15] R. A. Mastromauro, M. Liserre, T. Kerekes, and A. Dell' Aquila, "A single-phase voltage-controlled grid-connected photovoltaic system with power quality conditioner functionality," *IEEE Trans. Ind. Electron.*, vol. 56, no. 11, pp. 4436–4444, Nov. 2009.
- [16] J. M. Espí, J. Castelló, R. García-Gil, G. Garcerá, and E. Figueres, "An adaptive robust predictive current control for three-phase grid-connected inverters," *IEEE Trans. Ind. Electron.*, vol. 58, no. 8, pp. 3537–3546, Aug. 2011.
- [17] J.-M. Kwon, B.-H. Kwon, and K.-H. Nam, "Grid-connected photovoltaic multistring PCS with PV current variation reduction control," *IEEE Trans. Ind. Electron.*, vol. 56, no. 11, pp. 4381–4388, Nov. 2009.
- [18] S.-K. Kim, J.-H. Jeon, C.-H. Cho, J.-B. Ahn, and S.-H. Kwon, "Dynamic modeling and control of a grid-connected hybrid generation system with versatile power transfer," *IEEE Trans. Ind. Electron.*, vol. 55, no. 4, pp. 1677–1688, Apr. 2008.
- [19] S. V. Araújo, P. Zacharias, and R. Mallwitz, "Highly efficient single phase transformerless inverter for grid connected photovoltaic systems," *IEEE Trans. Ind. Electron.*, vol. 57, no. 9, pp. 3118–3128, Sep. 2010.
- [20] Y.-M. Chen, H.-C. Wu, Y.-C. Chen, K.-Y. Lee, and S.-S. Shyu, "The AC line current regulation strategy for the grid connected PV system," *IEEE Trans. Power Electron.*, vol. 25, no. 1, pp. 209–218, Jan. 2010.
- [21] M. Liserre, F. Blaabjerg, and S. Hansen, "Design and control of an LCLfilter- based three-phase active rectifier," *IEEE Trans. Ind. Appl.*, vol. 41, no. 5, pp. 1281–1291, Sep./Oct. 2005.
- [22] H. Bai, C. Mi, C. Wang, and S. Gargies, "The dynamic model and hybrid phase shift control of a dual active bridge converter," in *Proc. IECON*, 2008, pp. 2840–2845.
- [23] P. A. Dahono, "New hysteresis current controller for single-phase fullbridge inverters," *IET Power Electron.*, vol. 2, no. 5, pp. 585–594, Sep. 2009.
- [24] C. Mi, H. Bai, C. Wang, and S. Gargies, "Operation, design and control of dual H-bridge-based isolated bidirectional DC–DC converter," *IET Power Electron.*, vol. 1, no. 4, pp. 507–517, Dec. 2008